

Analysis of Solar Chimneys in Different Climate Zones - Case of Social Housing in Ecuador

Luis Godoy-Vaca¹, Manuel Almaguer¹, Javier Martínez-Gómez^{1,3},
Andrea Lobato¹ and Massimo Palme²

¹ Instituto Nacional de Eficiencia Energética y Energías Renovables, Quito, Ecuador

² Universidad Católica del Norte, Antofagasta, Chile

³ Universidad Internacional SEK Ecuador, Quito EC170134, Quito, Ecuador

luis.godoy@iner.gob.ec

Abstract. The aim of this research is to simulate the performance of a solar chimney located in different macro-zones in Ecuador. The proposed solar chimney model was simulated using a python script in order to predict the temperature distribution and the mass flow over time. The results obtained were firstly compared with experimental data for dry-warm climate. Then, the model was evaluated and tested in real weather conditions: dry-warm, moist-warm and rainy-cold. In addition, the assumed chimney dimensions were chosen according to the literature for the studied conditions. In spite of evaluating the best nightly ventilation, different chimney wall materials were tested: solid brick, common brick and reinforced concrete. The results showed that concrete in a dry-warm climate, a metallic layer on the gap with solid brick in a moist-warm climate and reinforced concrete in a rainy cold climate used for the absorbent wall improve the thermal inertia of the social housing.

1. Introduction

Solar energy has an important influence on energy consumption in buildings. The use of passive solar techniques in buildings, is a renewable alternative that can reduce annual (air conditioning) heating demand up to 25 % [1]. Some of these renewable architectural device are: solar chimneys, solar roofs and Trombe walls. Solar chimneys, which are also known as storage and solar heating walls, can reduce a building's energy consumption up to 30% [2]. An important bioclimatic architectural strategy for ventilation, heating and cooling of buildings are Trombe Walls which are built as part of the building façades.

Solar chimneys are systems of natural ventilation that use solar radiation to produce convective currents. The convective currents draw the air inside of the building requiring one or more solar chimneys to allow an enough heat income from the solar radiation to create the thermal buoyancy effect. As a result, an air temperature difference is created and a density gradient between the inside and the outside of the chimney is obtained, which induces a natural upwards movement of air. Its use depends on the weather, in moist-warm and dry-warm climates, solar chimneys are used to heat dissipation and produce, due to the air movement, a thermal comfort for people. [3]. The impact of the air movement decreases the temperature inside the house. Nevertheless, in rainy-cold climates, solar chimneys are used as heat accumulators to increase the temperature inside the house [4].

Solar chimneys development is a relative current fact [4]. Three types of researches or the combination of them have been utilized for the characterization of solar chimneys. Firstly, experimental researches helped to demonstrate and to corroborate different chimneys models and their equations, as shown by: performance [5] and dynamic and physical model [6] of solar chimneys investigations. Secondly, computational researches increase according to computational calculation power. Some authors use computational tools to validate solar chimney models aiming to avoid the construction of the solar chimney itself. With computer software, very close results to the real models ones are obtained,



as shown by: simulation and experiment [7], implementation [8] and numerical study [3] in solar chimneys works. Finally, with experimental and/or computational researches, analytics researches were obtained, too. Different equations were showed in this research which can be used to obtain the temperature distribution, mass and velocity air flow rate, as well as other solar chimneys' important variables [5] and [1].

A good example of the use of an analytic and experimental research was performed by [6]. This model was related to a dynamic-physical model applied to study the non-uniform temperatures distribution of a chimney, placed in warm-dry climates. The results were compared with a real system. Good results were obtained when testing the nocturnal ventilation by the effect of thermal inertia, using reinforced concrete for the wall. But few studies analyzed the performance of a solar chimney in hot humid climates. Sudprasert et al. [3] performed a study testing different heights and a reduced backward flow at the opening. The yield of ventilated airflow was 15.4 – 26.2% less than chimneys in dry-warm climates, while the overall air temperature was higher, for a solar chimney with moist air. On the other hand, [2] wrote a review of solar chimneys investigations inside the houses (Trombe walls) for heating, ventilation and cooling. He recommended 20 - 40 cm mass concrete as an absorber wall due to that fact that it absorbed energy much better. This type of solar chimney could improve the ambient temperature inside the house. This research indicated that solar chimneys could be a good alternative to improve thermal comfort inside the houses in any type of climate.

In Ecuador, the study carried out by [9] and [10] showed that over the last decade, the government has implemented several programs of social housing to reduce the quantitative housing deficit. The main social housing model has the same design and construction materials regardless the climatic zone. For this reason, the minimum living conditions related to thermal comfort in every region have not been achieved.

With this in mind, this study provides a research to improve indoor thermal comfort by using a solar chimney as a natural ventilation for social houses, in different climatic zones in Ecuador. A dynamic-physical model has been implemented in order to analyse the solar chimney performance. The proposed solar chimney model was simulated using a Python script in order to predict the temperature distribution and the mass flow over time. The results obtained were firstly compared with experimental data for dry-warm climate. Then, the model was evaluated and tested over real weather conditions: dry-warm, moist-warm and rainy-cold. In addition, the assumed chimney dimensions were chosen according to those recommended in literature for the studied conditions.

2. Methodology

The methodology includes a case study of a solar chimney in the literature in order to validate a dynamic-physical model. This model should obtain similar results in dry-warm climate. This model was programmed in Python software (modern programming language that is common use in scientific ambient and software develop) to obtain the temperature and mass flow rate evolution. Once the model was validated, this model was used to simulate the temperature and mass flow rate evolution for different macro-zones in Ecuador.

2.1. Case study

To evaluate the performance of a solar chimney in a warm climate, it is necessary to define dimensions and physical characteristics of the materials. The proposed dimensions correspond to the studies performed in dry warm climates by [6]. These values have been tested in several climates and they have achieved the best mass flow results.

These values will be useful to corroborate the mathematical model that will be programmed in Python. Once the dimensions of the chimney have been defined, the elements that constitute the chimney are described in table 1.

Two chimney configurations performed by [4] and [6] are showed in table 1. Configuration A used one material as absorbent wall. Configuration B used three different materials as absorbent wall. The absorbent wall was utilized as a heat accumulator for the night ventilation.

Only the glass properties were equal in the two configurations. It was assumed a glass thickness of 0.5 mm, an absorption coefficient (α_g) of 0.006; a transmissibility (τ_g) of 0.84; and an emissivity (ϵ_g) of 0.8. The inner surface of the wall was painted black. Therefore, the assumed solar radiation absorption (α_w) was 0.82.

In order to determine the number of intervals in which the wall is divided, the convergence criteria used the thermal diffusivity of the wall material, the period of time in which the values were obtained and the number of wall divisions were considered. The model was solved only using three points in order to reduce the simulation time. On the other hand, the period of time used to define the minimum interval of distance between each point was one hour since weather data used for the simulation had the same interval.

Table 1. Input properties of the solar chimney.

Climate Type	City of analysis	Chimney characteristics				
		Dimensions		Wall		
			Thickness=	Thermal conductivity (W/mk)	Heat capacity (J/KgK)	Density (Kg/m ³)
Dry-warm July 27-28, 2003 (Configuration A)	Almería, Spain	Height= 2m Channel width=20 cm Inlet and outlet areas= 0.025 m ²	24 cm Reinforced concrete			
			Total thickness=21 cm	Krc=1.63	Crc=1090	prc=2400
Dry-warm September 3-4, 2005 (Configuration B)	Almería, Spain	Height= 3m Channel width=20 cm Inlet area= 0.039 m ² Outlet area= 0.19 m ²	Reinforced concrete Mineral wool Wood flooring	Kmw=0.038 Kwf=0.14	Cmw=1674 Cwf=1700	pmw=30 pwf=600
Dry-warm, September, 13-14 of 2009 (Configuration A)	Guayaquil, Ecuador	Height= 2m Chanel width=14.5 cm Inlet and outlet areas= 0.025 m ²	24 cm Reinforced concrete	Krc=1.63	Crc=1090	prc=2400
Moist-warm September 11-12 of 2005 (Configuration B)	Nueva Loja, Ecuador	Height= 3m Chanel width=20 cm Inlet and outlet areas= 0.01 m ²	Total thickness=24 cm Metallic layer (ASTM A653 C5) Solid brick	Kml=42.3 Ksb=0.87	Cml=442 Csb=1330	pml=7848.5 pml=1800
Rainy-cold, September, 14-15 and 20-21 of 2005 (Configuration A)	Quito, Ecuador	Height= 2.5m Chanel width=14.5 cm Inlet and outlet areas= 0.025 m ²	30 cm Concrete	Kc=1.35	Cc=1000	pc=1800

To solve this equation system, it is necessary to take into consideration some aspects. Each new wall temperature depends on the temperature and heat transfer parameters at a previous time. For this case, the previous conditions for the first calculation (time 0) are not known, that is why, the wall temperatures ($T_o=308$ K, $T_1=307$ K, $T_{1s}=303$ K) are constant and equal to the conditions of [6].

At the same way, the environmental conditions such as: temperature, solar radiation, vertical surface and wind speed; are the same as [6] for dry and warm condition to Almería, Spain, every hour. The physical process involved in this model is presented in [4].

2.1.1 Model

The mathematical concepts that were used as baseline for creating this software are detailed in [4]. The solar chimney model was developed using the programming language python as shown by [13] in its version 3.4. The class design follows the Object Oriented Programming paradigm.

The multiple mathematical operations, that are performed following the model, were developed using the parallel programming tools of Python, which has many advantages as shown by [14]. In order to speed up the final result, the Python multiprocessing package, which allows to perform concurrent operations on Cpython's Global Interpreter Lock (GIL) was used. It also allows to exploit all the cores of the computer, which cannot be achieved using the threading package [14]. All the processes created shared a common queue, provided by the multiprocessing package, where they write the obtained results.

2.1.2 Variable Configuration

Before starting the simulation process it is necessary to configure the variables to be used in the software. Even though the solar chimney's default values are used, the variables that are part of the the solar chimney can be customized. The main variables are the properties of the wall, weather and glass.

The weather data to be used in the simulation can be read from the EPW files as well as from any plain text file in CSV format. It should be noted that, for CSV formatted text files, the position of each of the weather variables must be specified. EPW files contain one year of weather data. It can take a lot of time to simulate a whole year. The software allows to specify the range of time to do the simulations.

2.1.3 First Simulation Phase

The first phase of the simulation consists in finding the values of the following variables: Fluid Temperature (Tf), Glass Temperature (Tg) and Temperature of the Wall that is connected to the duct (To). For this, a range of variation is established for each of these variables and the increment for the variation is done in decimals. For each value, the calculation of the *approximation* (4) to 0 is performed by the following equation:

$$\text{approx} = Sg + (Hg * (Tf - Tg)) + (Hrwg * (To - Tg)) - (hwind * (Tg - Ta)) - (Hrgs * (Tg - Ts)). \quad (1)$$

The primary objective is to find an approximation value as close as possible to 0. This calculation is performed by processes implemented in Python simultaneously. When a process finishes, it is responsible for writing in the queue the best approximation value obtained and the combination of the variables To, Tg, Tf used to obtain the result. To carry out this operation, it is necessary to previously perform operations that solve the value of the variables involved in the equation, among which are solar radiation gain by the glass (*Sg*), transfer coefficient between wall and glass (*Hrwg*), transfer coefficient between the glass and the sky (*Hrgs*) and transfer coefficient between glass and air (*Hg*), which are shown [10].

For the calculation of *Hrwg* and *Hrgs*, it is necessary to use of the *SteffanBoltzmann* constant (σ), which has a value of $5.67 \times 10^{-8} \text{ W} \cdot \text{m}^{-2} \cdot \text{K}^{-4}$. The calculation of the variable *Hg* has dependence on variables that must be solved before being able to complete this calculation. First, the thermal conductivity glass-air (*kga*) variable can be solved.

The nusselt number for the surface glass-air (*Nuga*) value depends on the value that the Rayleigh number for the surface glass-air (*Raga*) variable takes, if *Raga* is less than 10^9 , other formula will be used for its calculation as shown [6].

Despite the previously used scenario, it is necessary to make use of the variables *Raga* and Prandtl number glass-air (*Prga*). The calculation of *Prga* and *Raga* variables introduces the glass-air properties Rayleigh number for the surface glass-air (*grga*), viscosity glass-air (*ufga*), specific heat glass-air (*Cpga*) and thermal conductivity glass-air (*kga*). In turn (*grga*) needs coefficient of expansion of glass-air (β_{ga})

and difference temperature glass-air (Δga). Where the variables mean temperature glass-air ($tmga$) and density (pga) are calculated.

All the calculations detailed above aim to find the approximate value closest to 0, which will be used in the second phase of the simulation together with the variables solar radiation gain by the wall (Sw), transfer coefficient between wall and air (Hw) and density wall-air (pwa), which must be still calculated.

The Nusselt number for the surface wall-air ($Nuwa$) value depends on the value of the variable Rayleigh number for the surface wall-air ($Rawa$), if $Rawa$ is less than 10^9 , other formula will be used for its calculation, whatever the scenario used previously, it is necessary to make use of the variables Prandtl number wall-air ($Prwa$) and $Rawa$. For the calculation of the variables $Prwa$ and $Rawa$, new variables such as specific heat wall-air ($Cpwa$), wall-air viscosity ($ufwa$) and Rayleigh number for the surface wall-air ($grwa$) must be obtained. In the previous formulas, new variables mean temperature wall-air ($tmwa$), coefficient of expansion of wall-air (βwa), difference temperature wall-air (Δwa) and $vfwa$ are introduced and they must be calculated. All process and formulas are shown in [6].

Each created process implements the calculations detailed above. All the necessary variables are obtained in order to continue the simulation process. The results of each process are written in a queue for further processing. Once all the processes have been completed, the best result obtained from each process is written in a new queue and sorted by their proximity to 0, regardless of whether they are positive or negative.

2.1.4 Mass flow

The mass flow is calculated out of the best values obtained in the previous process. In cases where $Tf - Ta$ is less than 0, the mass flow is assigned the value of 0. Otherwise its calculation is done by the following formula:

$$\text{Mass flow} = Cd * ((pwa * Aow) / \sqrt{(1 + Aow/Aiw)}) * \sqrt{((2 * g * Lw * (Tf - Ta)) / Ta)}. \quad (2)$$

2.1.5 Programming conditions

The best-obtained values are analysed. Some defined rules are applied with the objective of selecting the best value amongst all. The rules developed for this version of the software are hard coded. It is expected that the next version of the software will include capabilities for configuring and adjusting the rules per the preferences of each user. Each applied condition is weighted with a value. In case that a condition is fulfilled, the weights are added. Sorting in descending order based on the sum of the fulfilment of each condition allows to have in the first place the value that more rules have fulfilled.

The conditions were defined taking into consideration the opinion of field experts that are members of the project. To use an example, one of the applied rule is related to the Ta value, in case the Ta value undergoes a decrease, both the values of Tg and Tf are expected to decrease too. This series of conditionals helps the solar chimney in maintaining a logical and, to some extent, a predictable behaviour within the expected parameters.

2.1.6 Second Phase of the Simulation

First thing to do for the second phase of the simulation is to find the next value of the To variable. To represent the temperatures over time, the same variable is used and 1 is added at the end, so that To at the next instance of time is represented by $To1$. The formulas used in the second phase of the simulation are shown below.

$$To1 = ((Sw - (Hw * (To - Tf)) - (Hrwg * (To - Tg)) - ((Kfw / \Delta x) * (To - T1))) * ((2 * 3600) / (Cw * Pw * \Delta x))) + To \quad (3)$$

$$Hrws = (0.0000000567 * Ew) * (T15 + Ts) * (T15^2 + Ts^2) \quad (4)$$

Once the variable To have been solved in the next instance of time, the variables Tg and Tf are calculated. This time it is not necessary to vary To since it has already been resolved.

After the processes responsible for varying Tg and Tf are created, it begins a loop where all the operations described from the first phase of the simulation until now are repeated. The loop runs as many times as is specified in the variable configuration, where the time period defines the number of

iterations performed by the software. Each result obtained from the iterations is stored in a list, which is finally persisted to a plain text file. Other fact that be considered in the simulation programm was the possiibility to add two or more materials. When the chimney absorbent wall is analyzed with the addition of a new material, the program uses the equation below:

$$T_{m1} = \frac{(K_{m1} / \Delta x_{m1}) * (T_{i-1} - T_i) - (K_{m2} / \Delta x_{m2}) * (T_i - T_{i+1})}{\Delta x_{m1} / 2 + (3600 / ((P_{m1} * C_{m1} * \Delta x_{m1}) / 2 + (P_{m2} * C_{m2} * \Delta x_{m2}) / 2))} + T_i \tag{5}$$

2.1.7 Validation

After finishing the Python program, the obtained graphs were used to validate the dynamic physical model proposed by [4] as shown in figure 1 and 2, for the two configurations. It was concluded, during daytime the ambient temperature is higher than the glass temperature as is showed in figure 1-a and figure 2-a. The opposite occurs at night, where the ambient temperature decreases. Consequently, at a certain time, the ambient temperature is the same or lower than the glass temperature. The fluid temperature is higher than the ambient temperature in most of the time, except for a few hours when the ambient temperature and solar radiation are increasing. In the same figure 1, the temperature in the inner surface of the concrete wall was indicated too. It demonstrates that in the night hours the wall has thermal inertia. The air volume that crosses the chimney are presented in figure 1-b and figure 2-b. It reaches its maximum value at night. The volume air flow is superior to 0.010 Kg/s during most of the time of simulation in the two configurations, even at the same hours at [4] when they are nil around 11 am. These results allow the validation of the mathematical model.

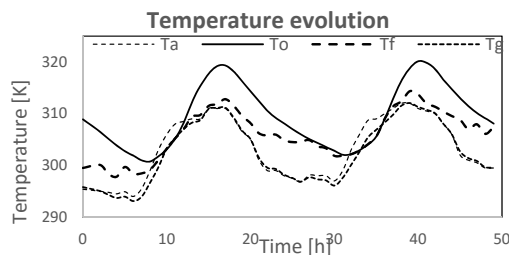


Figure 1-a. Temperature evolution with “A configuration”

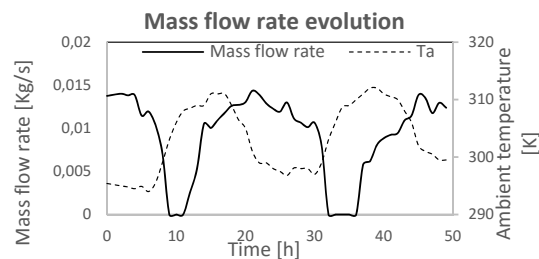


Figure 1-b. Mass flow rate evolution with “A configuration”

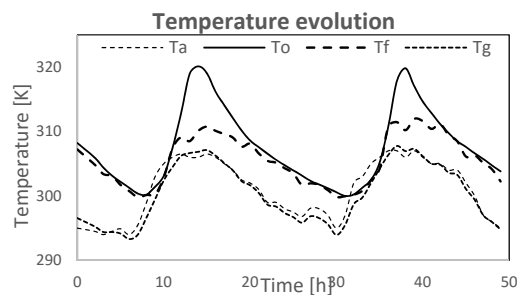


Figure 2-a. Temperature evolution with “B configuration”

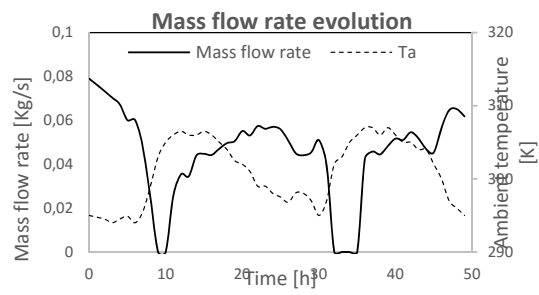


Figure 2-b. Mass flow rate evolution with “B configuration”

Once that the obtained results were very close to the studied ones, it is possible to enter into the Python program a climatic file that should contain: solar radiation, ambient temperature and wind speed, as well as constructive aspects and properties of the materials, to obtain the distribution of temperatures and mass flow over time.

2.2 Experimentation

A real weather data series from a meteorological station, corresponding to two days of measurements. These days were selected when the incident solar radiation was complete with clear sky conditions. Data were recorded in Guayaquil, Quito and Nueva Loja, Ecuador. These three representative cities were selected for each macro climatic zone in Ecuador as shown in [9] and [10]. The data of the two

consecutive days correspond to the constant and the highest values of solar radiation and environmental temperature. Furthermore, the measured wind speed had the lowest values at noon. These data were hourly recorded and represented in figures 3, 4 and 5.

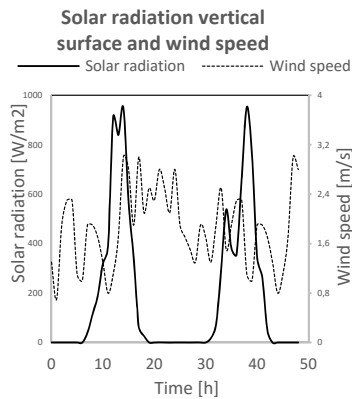


Figure 3. Weather real data, corresponding to two days in Guayaquil, Ecuador

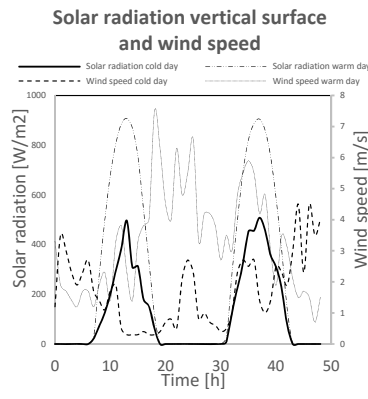


Figure 4. Weather real data, corresponding to two days (two colds and two warm days) in Quito, Ecuador

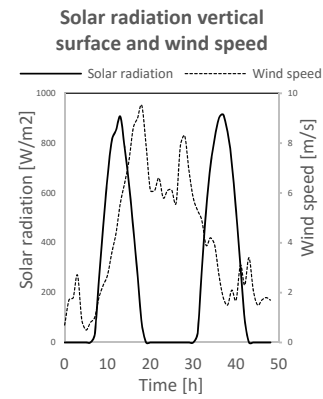


Figure 5. Weather real data, corresponding to two days in Nueva Loja, Ecuador

From the results presented by [4] to dry-warm climate, [3] to moist-warm climate and [2] to rainy-cold climate, the same dimensions and walls properties of each chimney were collected for the current analysis as is presented in table 1. With these values and climatic data for each macro-zone, a different configuration was tested in the software. In this work, the most frequently used materials for solar chimney walls construction were analyzed. It is important to clarify that in rainy-cold climate (Quito) a solar chimney inside the house as a Trombe wall was considered. An important fact considered in this work was that the solar chimney in this climate could work as a solar chimney and as a Trombe wall as well, just by opening or closing the indoor or outdoor Gates, according to the user requirements. These two gates could be installed in the top of the chimney.

The configuration considered was the west orientated vertical chimney, since the highest solar radiation occurred in the afternoon and the chimney is located near the equator. On the other hand, fabrication costs for vertical configurations are lower than costs for inclined configurations.

3. Results

3.1 Temperatures evolution

The temperature evolution profile is shown in Figure 6-a, 7-a and 8-a. It can be observed that the highest wall temperature is reached when the ambient temperature is also the highest. At the same time in these figures can be observed that the ambient temperature (T_a) with the glass temperature (T_g) follow a similar or a very close profile. Something similar occurs between wall temperature (T_o) and fluid temperature (T_f), which can follow similar temperature profiles most of the time, but the fluid temperature is more sensible to the variation of weather conditions such as wind speed or solar radiation.

3.2 Mass flow rate evolution

Figures 6-b, 7-b and 8-b show the evolution of mass flow rate. It can be observed that a mass flow exists in all climates. This fact indicates that the solar chimney works with different weather conditions. These figures indicate the correlation between T_o , T_f and the mass flow rate. A high ambient temperature and solar radiation can produce a high T_o and T_f . T_o and T_f are responsible for the increase or decrease of the mass flow rate. When the values of T_o and T_f are both similar and high, a higher mass flow rate is achieved, which is beneficial for a good chimney performance.

Figure 6-b indicates the mass flow rate evolution of the chimney in dry-warm climate. This behaviour is similar of the figure 1-b for the similar weather conditions where most of the time its mass flow rate

is more than 0.01 (Kg/s). This value represents a wind speed inside a house around 0.34 (m/s) and could be positive at night, when the indoor wind speed decreases due to the closed windows and doors for security reasons. Moreover, the exterior wind speed is lower at night, too. As shown in [11], a value of indoor wind speed around 0.04 (m/s) could decrease the indoor temperature by 2 - 3°C, but, according to this author, a higher air velocity around 2 (m/s) or 0.058 (Kg/s) is recommendable in order to feel an important temperature decrease inside the house. This air motion could be increased by installing several free openings in the house next to the solar chimney.

Figure 7-b shows the results of the two different uses of the solar chimney. The first one is the performance of the mass flow rate of the solar chimney when the solar radiation and ambient temperature show the highest values. With these weather conditions a high mass flow rate was obtained, compared to the rate obtained for lower ambient temperatures and lower solar radiation. On the other hand, when a cold day shows decreases of ambient temperature, solar radiation and wind speed, a good performance of the solar chimney (Trombe wall) is obtained, too.

Figure 8-b shows lower values of mass flow than those obtained in dry-warm conditions. It could be possible due to moist air and a high wind speed. This is why, in this type of climates, it is recommended to use a metal layer next to solid brick as material construction in the wall. The galvalume (ASTM A653 C5 steel) as metal layer, helps to increase the gap temperature to evaporate the water percentage, rapidly as shown in [12], while the solid brick accumulates the heat for the night ventilation as shown in [7].

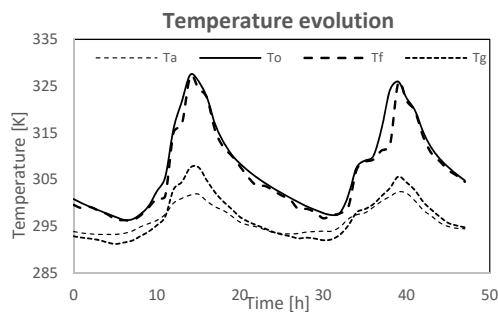


Figure 6-a. Results of evolution of temperatures in Guayaquil

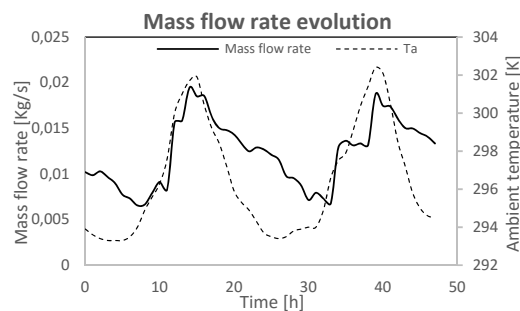


Figure 6-b. Results of evolution of mass flow rate in Guayaquil

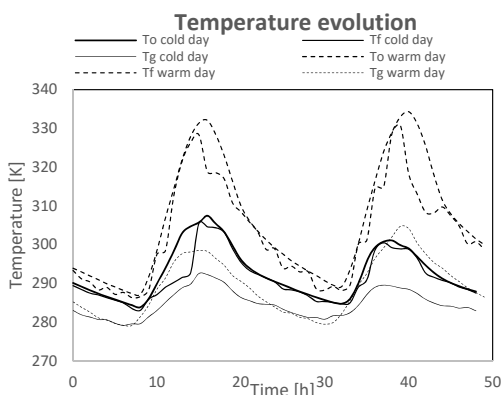


Figure 7-a. Results of evolution of temperatures in Quito

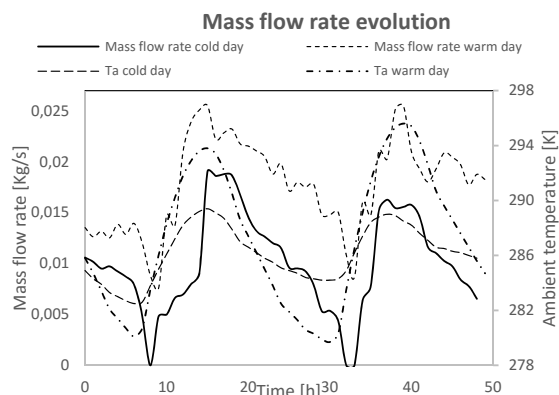


Figure 7-b. Results of evolution of mass flow rate in Quito

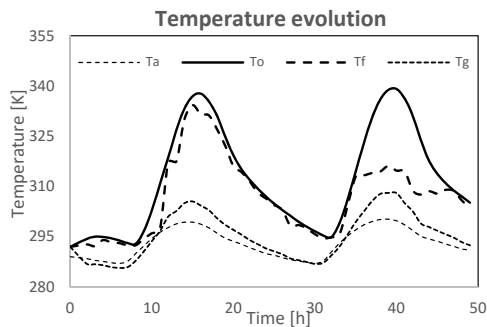


Figure 8-a. Results of evolution of temperatures in Nueva Loja

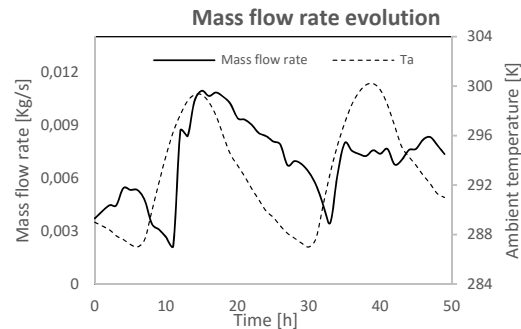


Figure 8-b. Results of evolution of mass flow rate in Nueva Loja

4. Discussions of results

The proposed dynamic physical model was validated. It showed consistent results that were similar to the studies carried out by [6] and [4]. This mathematical model was programmed in Python software to obtain glass, fluid and wall temperature evolution as well as the mass flow evolution. The variables input to the program were: climatic data, dimensions of the chimney and properties of different construction materials.

In order to observe the behaviour of the solar chimney in different macro-zones in Ecuador, the input data for the program were the real weather data of Guayaquil, Quito and Nueva Loja. These zones have particular weather conditions: dry-warm in Guayaquil, rainy-cold in Quito and moist-warm in Nueva Loja. These factors determined the importance of a solar chimney for a house, because the chimney allows not only to decrease both the temperature and the relative humidity rate inside the house in warm climates but also, to create greater airflow changes that lead to a healthier ambient.

For rainy-cold climates as Quito, it could be possible to have two different uses for the solar chimney. At the top of the chimney, gates can be added. The roof gate could be utilized when the ambient temperature is high and it is necessary to remove “hot air” from the inside of the house. On the other hand, when the ambient temperature inside the house is low, it could be possible to close the roof gate and to open the inside gate to introduce a warm air as an effect of the solar convection in the chimney.

Another important variable in these zones to take into account was the difference in weather conditions. For each weather condition, the solar chimney should have specific dimensions to improve its performance. Also, an important parameter is the wall material that will perform as heat accumulator. According to literature, it is important for the temperature inside the shaft to be the highest possible. This condition improves the thermic buoyancy effect and thus, a bigger mass rate is obtained. In addition, accurate material picking for the insulating wall causes a positive effect of thermal inertia that improves night time ventilation.

Once that the required input data such as environmental conditions, dimensions and materials characteristics were provided, the program showed the profile temperature and flow mass versus time functions for each analysed climatic zone. It could be useful to determine the chimney performance in different climate zones and to make the decision whether to incorporate a solar chimney in a social house or not. In social housing in Ecuador, as shown by [9] and [10], the indoor thermal environment is generally within the range of thermal comfort because the construction materials of the social house are the same regardless the climatic zone.

5. Conclusions

The obtained results in the present study permitted to observe the best material performance for a solar chimney. Considering that Ecuador has three different climatic macro-zones, the solar chimney performance was simulated using different absorbent wall materials to determine the best configuration and wall material for each macro-zone. The results showed that, for a dry-warm climate, it is better to

use concrete for the absorbent wall; for a moist–warm climate, the absorbent wall consists of a metallic layer on the gap with solid brick; and finally, for a rainy cold climate, it should be used reinforced concrete for the absorbent wall. These wall materials correspond to those from a literature compilation, considering that these materials will be beneficial at night, when heat is discharged. In fact, the heat absorbed during the day is not transferred to the house. These materials could be used at the same time as heat absorbing material and as insulating material.

References

- [1] Liu S, Liu J, Yang Q, Pei J, Lai D, Cao X, et al. Coupled simulation of natural ventilation and daylighting for a residential community design. *Energy Build* [Internet]. 2014;68:686–95. Available from: <http://dx.doi.org/10.1016/j.enbuild.2013.08.059>
- [2] Saadatian O, Sopian K, Lim CH, Asim N, Sulaiman MY. Trombe walls: A review of opportunities and challenges in research and development. *Renew Sustain Energy Rev* [Internet]. 2012;16(8):6340–51. Available from: <http://dx.doi.org/10.1016/j.rser.2012.06.032>
- [3] Sudprasert S, Chinsorranant C, Rattanadecho P. International Journal of Heat and Mass Transfer Numerical study of vertical solar chimneys with moist air in a hot and humid climate. *Int J Heat Mass Transf* [Internet]. 2016; 102:645–56. Available from: <http://dx.doi.org/10.1016/j.ijheatmasstransfer.2016.06.054>
- [4] Martí-Herrero J. Solar chimney characterization through physical parameters such as natural ventilation system (spanish). National university of distance education (Spain); 2006.
- [5] Ong KS, Chow CC. Performance of a solar chimney. *Sol Energy*. 2003; 74:1–17.
- [6] Martí-Herrero J, Heras-Celemin MR. Dynamic physical model for a solar chimney. *Sol Energy*. 2007; 81:614–22.
- [7] Afonso C, Oliveira A. Solar chimneys: simulation and experiment. *Energy Build*. 2000; 32:71–9.
- [8] Chung P, Ahmad MH, Ossen DR, Hamid M. Implementation of Solar Chimney in Orang Asli Settlement in Bukit Lagong, Selayang. In: 5th International Graduate Conference on Engineering Science & Humanity. Johor Bahru, Malaysia; 2014. p. 1–7.
- [9] Gallardo A, Palme M, Beltrán D, Lobato A. Analysis and Optimization of the Thermal Performance of Social Housing Construction Materials in Ecuador. In: International Conference on Passive and Low Energy Architecture Cities, Buildings, People: Towards Regenerative Environments [Internet]. Los Angeles: PLEA 2016; 2016. Available from: <https://www.researchgate.net/publication/305462556>
- [10] Palme M, Lobato A. Robustness of social houses in Ecuador facing global warming: prototyping and simulation studies in the macroclimatic regions of Amazons, Coast and Andes. In: Mediterranean Green Buildings and Renewable Energy Forum. Florence; 2015.
- [11] Khedari J, Boonsri B, Hirunlabh J. Ventilation impact of a solar chimney on indoor temperature fluctuation and air change in a school building. 2000; 32:89–93.
- [12] Chungloo S, Limmeechokchai B. Application of passive cooling systems in the hot and humid climate: The case study of solar chimney and wetted roof in Thailand. 2007; 42:3341–51.
- [13] Palach, J. *Parallel Programming with Python*. Packt Publishing. 2014. Ltd.1-106.
- [14] Friborg, R. M., Bjondalen, J. M., & Vinter, B. Three Unique Implementations of Processes for PyCSP. 2009, November. P. 277-292.

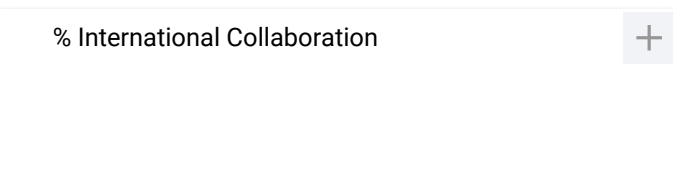
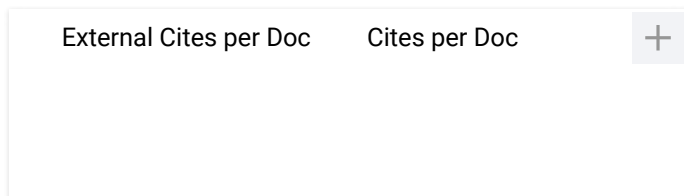
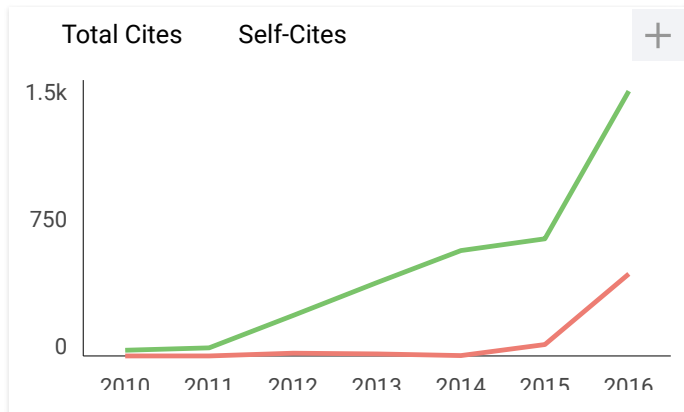
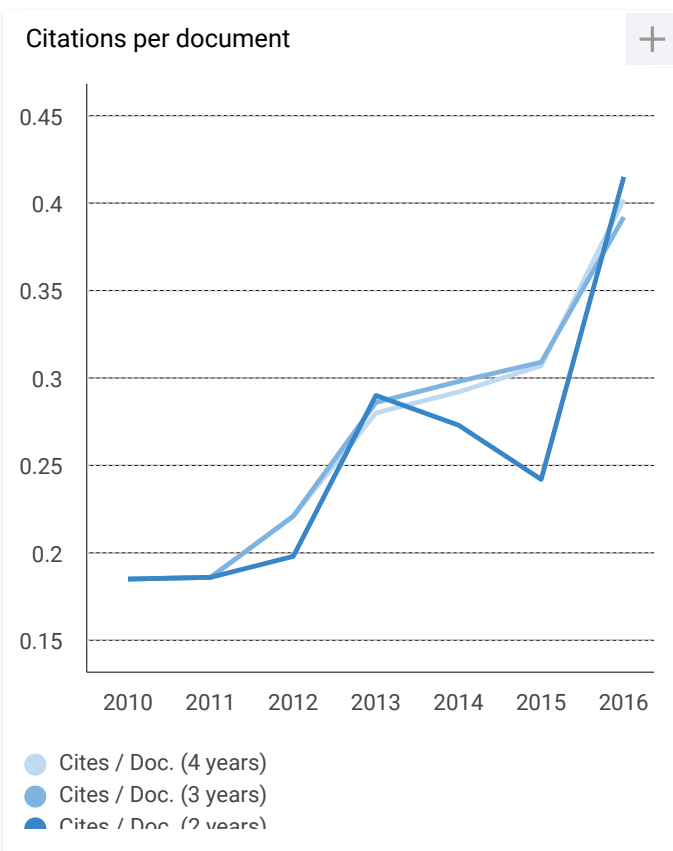
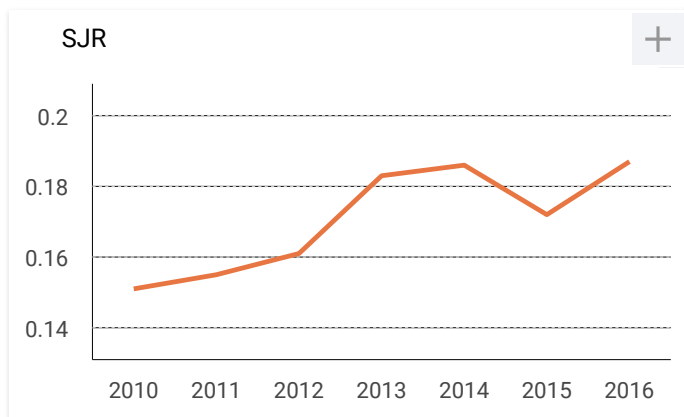


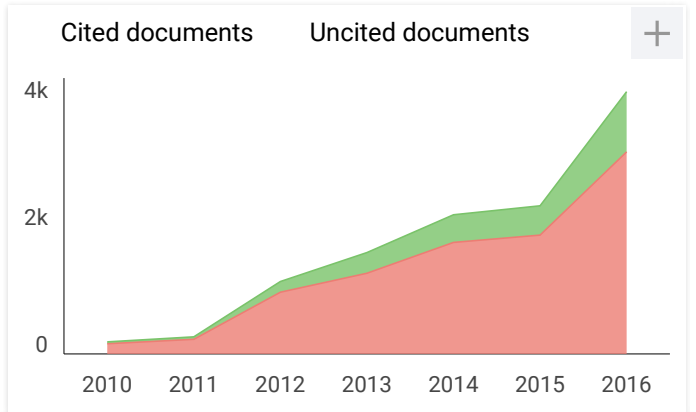
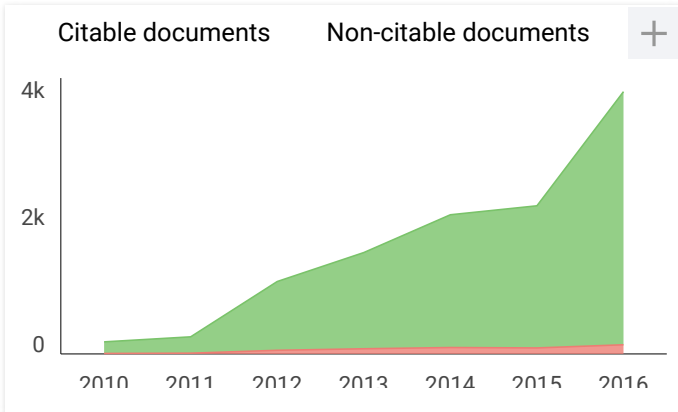
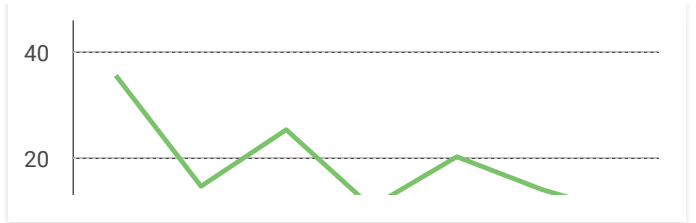
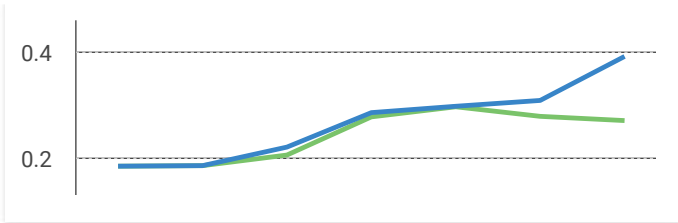
IOP Conference Series: Materials Science and Engineering

Country	United Kingdom
Subject Area and Category	Engineering Engineering (miscellaneous) Materials Science Materials Science (miscellaneous)
Publisher	
Publication type	Conferences and Proceedings
ISSN	17578981
Coverage	2009-ongoing

13

H Index





IOP Conference Series: Materials Science and Engineering

Indicator	2009-2016	Value
SJR		0.19
Cites per doc		0.41
Total cites		1440

www.scimagojr.com

← Show this widget in your own website

Just copy the code below and paste within your html code:

```
<a href="http://www.scimagr
```

Developed by:



Powered by:



Follow us on Twitter

Scimago Lab, Copyright 2007-2017. Data Source: Scopus®

